International Scholarly Research Network
ISRN Materials Science
Volume 2011, Article ID 857432, 5 pages
doi:10.5402/2011/857432

Research Article

Crystal Structure of Locally Available Tassar Fibers Based on $[Ala\text{-}Gly]_n$ Amino Acid Sequence: Using X-Ray Data and LALS Method

Parameswara Puttanna and Somashekar Rudrappa

Department of Studies in Physics, University of Mysore, Manasagangotri, Mysore 570006, India

Correspondence should be addressed to Somashekar Rudrappa, rs@physics.uni-mysore.ac.in

Received 12 April 2011; Accepted 9 May 2011

Academic Editors: M. Celino, Y. X. Gan, and Y. Sun

X-ray diffraction pattern from locally available Tassar fibers was recorded using imaging plate system (Dip-100S). The pattern was used along with fiber processing software to identify the reflections and to compute X-ray intensities. A molecular model was first constructed with standard bond lengths and angles using helical symmetry and layer-line spacing observed in the X-ray pattern. The model was then refined against observed X-ray data using linked-atom least-squares (LALS) method. The crystal and molecular structure of Tassar fibers is reported. It is concluded that the sheet structures formed by hydrogen bonds assume the antipolar-antiparallel arrangement.

1. Introduction

Silk is a composite material and generally defined as protein polymers that are spun into fibers by some Lepidoptera larvae such as silkworms, spiders, mites, and flies. Silk fibers are paracrystalline in nature and they have found extensive applications in textile industry. Compared to cellulose and other synthetic polymers, silk is peculiar for its durability, high strength, luster, and other unique features [1]. Among the Lepidopterans, the silk moths, especially *Bombyx mori*, *Antheraea pernyi*, *Antheraea mylitta,* and *Antheraea assama* play an important role in rural economy of many developing nations [2]. The importance of silk protein increased because of its potential use as a natural biopolymer for tissue engineering and biomedical applications. There are two classes of silk, namely, mulberry (*Bombyx mori*) and nonmulberry (Tassar, Eri and Muga). *Antheraea mylitta* (*A. mylitta*) is one of the wild varieties of non-mulberry silkworm, which produces Tassar silk. Few other wild silks are Mopani silk from South Africa, Saturniidae silk from Thailand, Assam silks (Muga, Eri, and Pat) from India, Tussah Silk from China, and Tassar Silk from India. Six million people in India alone are involved in sericulture, and one of the most economically important species for sericulture in India is the wild type nonmulberry silkworm, *A. mylitta* [2]. Tassar is a multivoltine type of silk and is mostly produced by tribal by rearing silkworms on forest plants (*Terminalia arjuna, Terminalia tomentosas* and *Shorea robusta*) [3]. Tasar silk fiber has its own distinctive color, is coarse to feel, but has higher tensile strength, elongation, and stress-relaxation values than the mulberry silk fiber secreted by *Bombyx mori*.

Different techniques were used by many researchers to understand the crystal and molecular structure of domestic and wild silk fiber varieties. Crystal structure of silk fibroin was reported by Marsh et al. who revealed that silk is made up of regular arrangements of antiparallel sheets [4]. Amino acid sequence, basic building blocks, of silk fibers, has been reported by number of researchers [5]. Refined molecular and crystal structure of Silk I base on Ala-Gly peptide sequence was carried by Okuyama et al. [6]. Crystal structure of pure Mysore silk (PMS) was carried out by Sangappa et al. [7]. Crystal and molecular structures of raw Bivoltine silk fibers were carried out by Mahesh and Somashekar who reported the comparison of parameters with pure Mysore silk fiber [8]. A rough computation of crystal structure of Tassar fiber in wet and dry condition was carried out by Reddy and

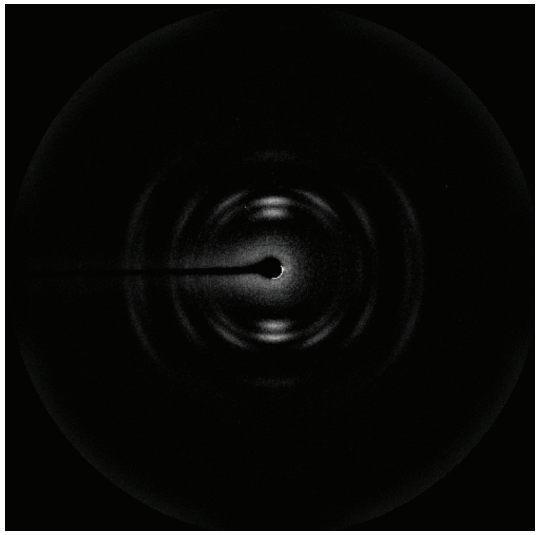

Figure 1: Background corrected X-ray diffraction pattern of Tassar silk fiber (bivoltine, nonmulberry).

others to find reason for two-load build-up regions in tensile graph [9].

In the present study, an attempt has been made to emphasis on modifications in crystal and molecular structure of Tassar silk (Indian) fibers employing X-ray diffraction data and linked-atom least-squares (LALS) refinement modeling, so that one can have a better perspective of structure property relation in these fibers.

2. Experimental

2.1. Sample Preparation. Locally available raw Tassar silk fibers belonging to *Antheraea mylitta* family, which comes under the classification multivoltine on the basis of shape, color, denier and life cycle of the fibers/cocoons. Cocoons were collected from the germ plasma stock of the Department of Sericulture, University of Mysore, which were then cooked in boiling water (100°C) for 2 min and transferred to water bath at 65°C for 2 min. Then the cocoons were reeled in warm water with the help of mono cocoon reeling equipment Epprouvite. These fibers were mounted on rectangular frame in *just taut* condition. The whole process, starting from reeling to mounting of fibers, does not involve any type of mechanical deformation.

2.2. X-Ray Diffraction Measurement. XRD patterns from raw Tassar silk fibers were recorded on an imaging plate. A rotating anode X-ray generator (ULTRA-X, RIGAKU) was operated in a normal focus mode to provide a monochromatic beam of wavelength ($\lambda = 7107$ Å), at 50 kV and 250 mA. Diffraction data was recorded on a disk-shaped imaging plate with the sample to plate distance of 150 mm. The measurement of X-ray diffraction data was implemented by the hardware system DIP100S (MACSCIENCE). The intensity values were thereby converted into pixel data in a rectangular coordinate system. A whole area of the imaging plate (diameter ~200 μm) was divided into 1600 × 1600 pixels each of a size of 125 mm^2. For this purpose, the program available in CCP13 suite was used (CCP13, 2004). For computation, a workstation, OCTANE, version 6.5 with an operating system IRIS 64, was used. Ivanova and Makowshi's (1998) method for background estimation, which is more reliable and consistent, was adopted [10]. It makes use of the fact that the background of a fiber diffraction pattern is typically composed of lower spatial frequencies than the diffraction maxima. Image plate X-ray pattern for Tassar fiber is given in Figure 1.

Each diffraction spot was picked by positioning the mouse on its centre, and coordinates were measured using SUN SP/2, a SUN microsystem Computer Corporation Business. After determining the centre and inclination angle of the X-ray pattern, the interplanar spacing was obtained by averaging the distances between the centre of the diffraction pattern and the positions of two or four equivalent reflections. The dimensions of unit cells were determined by least-squares method with the preliminary cell dimensions being obtained by a trial and error method on the computer display. We found no significant variation in the cell parameters of different silk fibers. The averaged cell parameters are $a = 9.44(5)$ Å, $b = 10.66(3)$ Å, and $c = 6.95(7)$ Å. The space group of the structure being $P2_12_12_1$ and has four asymmetric units in a cell each comprising two residues. The whole pattern fitting is carried out in two stages. In the first stage, X-ray diffraction pattern taken on a flat imaging plate system was transformed to reciprocal space using the specimen to film distance, rotation of image,

Table 1: Refined parameters of Tassar silk fiber with $[\text{Ala-Gly}]_n$ repeating unit.

Refined parameters	Tassar (*Antheraea mylitta*)
Torsional angles (°)	
φ_{Ala}	−141.76
ψ_{Ala}	148.44
ω_{Ala}	179.06
φ_{Gly}	−146.16
ψ_{Gly}	138.52
ω_{Gly}	177.87
Eularian angles (°)	
ε_x	−86.70
ε_y	126.71
ε_z	−142.01
Other parameters	
μ (°) chain-a	102.53
μ (°) chain-b	147.65
u(a); v(a); w(a)	0.7045; −3.5145; 0.5856
u(b); v(b); w(b)	1.5278; 1.5305; 0.3205
Scale factor	1.17
Attenuation factor	−4.83
R-factor	
R_N	0.330
R_w	0.390

Table 2: Observed (F_o) and calculated (F_c) structure amplitudes for (Ala-Gly) repeating unit.

Data Number	h	k	l	Multiplicity Factor	F_c	F_o
1	0	1	0	2	40.21	95.82
2	1	0	0	2	144.80	109.36
3	1	1	0	2	124.16	99.38
4	0	2	0	2	127.00	133.92
5	2	1	0	4	147.73	197.27
6	1	3	0	4	59.07	34.15
7	3	0	0	2	74.75	25.89
8	3	2	0	4		
9	1	4	0	4	62.87	119.13
10	4	1	0	8	32.11	24.89
11	4	2	0	4	64.57	40.82
12	0	5	0	2	48.16	48.74
13	1	5	0	4	63.04	66.01
14	3	4	0	4	80.18	95.33
15	0	2	1	2	45.62	60.59
16	2	1	1	4	37.60	128.47
17	3	0	1	2	38.39	27.99
18	3	1	1	4	19.38	38.99
19	2	3	1	4	57.66	40.32
20	3	2	1	4		
21	1	4	1	4	68.57	28.93
22	3	3	1	6	44.09	42.73
23	4	1	1	8	56.96	46.66
24	4	2	1	4	60.14	72.61
25	0	5	1	2	72.74	87.49
26	0	2	2	2	43.24	62.06
27	2	0	2	2		
28	2	1	2	4	66.94	33.65
29	2	2	2	6	77.46	28.25
30	1	3	2	4	21.18	25.28
31	3	0	2	2		
32	2	3	2	4	37.36	33.61
33	3	2	2	4		
34	1	4	2	4	84.18	79.39
35	1	1	3	4	40.04	33.18
36	0	2	3	2	27.63	49.96
37	2	1	3	4	91.74	97.29

wavelength, and tilt of the system and employing a program FTOREC, available in the software suite CCP13. In the second step, for the whole pattern fitting, we have used a program LSQINT available in CCP13 suite for which the input file is the output of FTOREC program. By inputting unit cell parameters, the space group symmetry, and the profile parameters, further processing of the pattern was carried out. Using CCP13 package "XCONV" with appropriate file options suitable for DIP image system, we can simulate cylindrical image and also calculate the integrated intensities with standard deviations [11]. The output of this routine give simulated cylindrical pattern and computed integrated intensities. These intensities were corrected for polarization and the Lorentz factors [12]. The output file which contains the integrated intensities corresponding to various (hkl) reflections with standard deviations are further used to determine the molecular and crystal structures of Tassar silk fibers.

3. Structure Determination

3.1. Molecular Model. Silk is a composite material with amino acid sequence as its primary structure. Amino acid analyses of *Antheraea* fibroins [5, 12] show a uniformly high content of alanine ($[\text{Ala}]_n$). There is an option in linked-atom least-squares (LALS) program to indicate two molecular chains by defining the constrains for only one of them. Here, the geometry for Ala is for the D-Ala and not L-Ala. The molecular conformation must satisfy both the sterical and mathematical requirements. Hence, we have chosen initial φ and ψ for Ala and Gly residues to be the same as that of Marsh et al. (1955) results [4], and the main chain was constructed with appropriate helical parameters together with bond lengths and angles.

Takahashi et al. (1999) have shown that there are four models for the sheet structure formed by hydrogen bonds. They are (i) polar-antiparallel [PA (1)]; (ii) polar-parallel (PP); (iii) antipolar-antiparallel (AA); (iv) antipolar-parallel (AP). In the polar model, the methyl groups of alanine residues are on one side of the sheet only. While in the antipolar model, the methyl groups alternately point to both sides of the sheet along the hydrogen bonding direction [13]. For the positioning of the molecular model in the unit cell, two additional parameters were used to define the relative axial rotation (μ) and translation (w) along the c-axis. At each stage in the modeling and refinement of the structure, we minimized the quantity Ω in the following least-squares fashion [14]. The first summation in Ω ensures the optimum agreement between the observed (F_o) and the calculated (F_c) X-ray structure amplitudes. The w is the weight of each reflection. The second

$$\Omega = \sum w(|F_o| - |F_c|)^2 + S\sum_j \in_j + S\sum_h \lambda_h G_h \qquad (1)$$

ensures the optimization of noncovalent interatomic ($\in_j$). S is the scale factor used to adjust the overall weight of the second term with respect to the first. Third imposes, by the method of Lagrange undetermined multipliers (lh), the exact constraints (Gh) we have chosen the exact constraints (Gh). Atomic scattering factors for calculating structure factors were obtained using the method and values given in International Tables for X-ray Crystallography (1974). Computations were carried out and compiled the LALS program using LINUX operating system based PC.

3.2. Molecular and Crystal Structure for Repeating Unit. The refinement was carried out for the crystal structure in which two antiparallel molecules related by a 2-fold rotation axis parallel to c-axis. In order to get appropriate packing parameters, the discrepancy factors R_c (conventional R factor) and R_w (weighted R_c factor) and shortest contact

Table 3: Fractional atomic coordinates of Tassar silk fiber for the repeating unit of (Ala-Gly).

Atom	Chain-a			Chain-b		
	x	y	z	x	y	z
Ala						
N	0.237	0.653	0.060	0.262	0.346	0.560
H_N	0.247	0.747	0.050	0.252	0.252	0.550
C_α	0.272	0.581	0.231	0.227	0.418	0.731
C_β	0.431	0.557	0.237	0.068	0.442	0.737
H_α	0.219	0.499	0.224	0.280	0.500	0.724
C'	0.228	0.654	0.411	0.271	0.345	0.911
O	0.230	0.770	0.413	0.269	0.229	0.912
Gly						
N	0.188	0.583	0.559	0.311	0.416	1.059
H_N	0.186	0.489	0.556	0.313	0.510	1.056
C_α	0.147	0.644	0.737	0.352	0.355	1.237
$H_{\alpha1}$	0.041	0.655	0.740	0.458	0.344	1.240
$H_{\alpha2}$	0.193	0.728	0.748	0.306	0.271	1.248
C'	0.189	0.566	−0.085	0.310	0.433	0.414
O(2)	0.183	0.464	−0.066	0.316	0.535	0.433

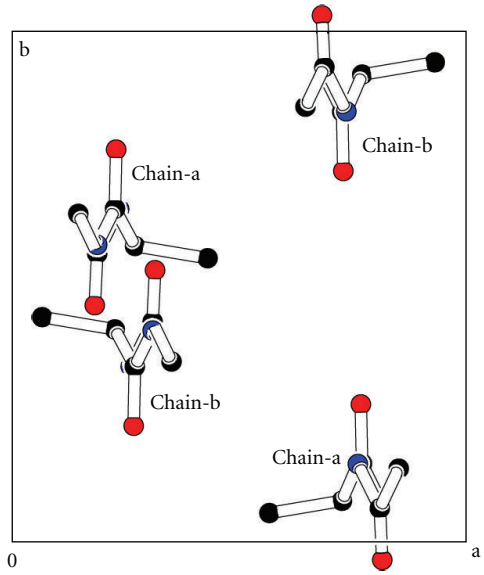

Figure 2: Down the fiber axis projection of crystal structure of Tassar silk.

between nonbonded atoms were calculated. Here, R_c and R_w were defined by

$$R = \sum \frac{||F_o| - |F_c||}{\sum |F_o|},$$
$$R_w = \sum \frac{w(|F_o| - |F_c|)^2}{\sum F_o^2}. \quad (2)$$

A dipeptide Ala-Gly was used as chemical repeating unit for refinement. The weight of each reflection "w" was fixed to 1.

4. Results and Discussion

The refined parameters and the final values are summarized in Table 1. Here, the azimuthal angles of the two molecules forming a sheet were also refined independently. The refinement gave good agreement between the observed and calculated structure factors (Table 2). Fractional atomic coordinates for (Ala-Gly) residues are given in Table 3. The crystal structure of Tassar silk in raw form is shown in Figure 2. The internal rotation angles (ω) of glycine and alanine residues about N–C(=O) bonds are 179.06 and 177.87, respectively, which are nearly *trans* conformation. The φ and ψ for the glycine residue are −146.16 and 138.52, respectively, which are also between *skew* and *trans* conformations. The φ and ψ for the alanine residue are −141.76 and 148.44, which respectively are in agreement with the values ($\varphi = -146.67^\circ$ and $\psi = 143.00^\circ$) given by Pauling and Corey for antiparallel-chain model [15, 16]. The torsional angles and Eulerian angles are the same for both chain-a and chain-b as they are symmetric. The steriochemical energy which is represented by σ is found to be $2.37E + 04$. Here the σ is given by the sum of second term of (1) [6]. We observe that the molecular modification is essentially same as β-pleated structure with antipolar-antiparallel arrangements formed by hydrogen bonds.

5. Conclusions

Crystal and molecule structure of locally available Tassar fiber, belonging to *A. mylitta* family, was carried out by X-ray diffraction data and employing linked-atom least-squares method. Four molecular chains are contained in the rectangular unit cell with parameters $a = 9.44$ Å, $b = 10.64$ Å, and $c = 6.95$ Å and the space group being $P2_12_12_1$. From the obtained values of torsional angles, Eulerian angles

and other parameters, we conclude that, in raw Tassar silk fiber, the sheet structures formed by hydrogen bonds assume the antipolar-antiparallel arrangement, which is in conformity with the results of Takahashi et al. (1999) [13].

References

[1] N. Reddy and Y. Yang, "Structure and properties of cocoons and silk fibers produced by Hyalophora cecropia," *Journal of Materials Science*, vol. 45, no. 16, pp. 4414–4421, 2010.

[2] S. Maity, S. I. Goel, S. Roy et al., "Analysis of transcripts expressed in one-day-old larvae and fifth instar silk glands of tasar silkworm, antheraea mylitta," *Comparative and Functional Genomics*, vol. 2010, article 246738, 2010.

[3] G. P. Singh, S. B. Zeya, A. K. Srivastava, B. Prakash, N. G. Ojha, and N. Suryanarayana, "Susceptibility of three eco-races of tropical tasar silkworm to *Antheraea mylitta* cytoplasmic polyhedrosis virus (AmCPV)," *Caspian Journal of Environmental Sciences*, vol. 6, no. 2, pp. 161–165, 2008.

[4] R. E. Marsh, R. B. Corey, and L. Pauling, "An investigation of the structure of silk fibroin," *Biochimica et Biophysica Acta*, vol. 16, pp. 1–34, 1955.

[5] F. Lucas and K. M. Rudall, in *Comprehensive Biochemistry*, M. Florkin and E. H. Stotz, Eds., vol. 26, p. 475, Elsevier, Amsterdam, The Netherlands, 1968.

[6] K. Okuyama, R. Somashekar, K. Noguchi, and S. Lchimura, "Refined molecular and crystal structure of silk I based on Ala-Gly and $(Ala\text{-}Gly)_2$-Ser-Gly peptide sequence," *Biopolymers*, vol. 59, no. 5, pp. 310–319, 2001.

[7] Sangappa, S. S. Mahesh, and R. Somashekar, "Crystal structure of raw pure Mysore silk fibre based on $(Ala\text{-}Gly)_n$-Ser-Gly peptide sequence using Linked-Atom-Least-Squares method," *Journal of Biosciences*, vol. 30, no. 2, pp. 259–268, 2005.

[8] S. S. Mahesh and R. Somashekar, "Crystal and molecular structures of raw bivoltine silk fibre—a comparative study," *Indian Journal of Fibre and Textile Research*, vol. 32, no. 2, pp. 143–149, 2007.

[9] T. Reddy, S. Roy, Y. Prakash et al., "Stress-strain curves and corresponding structural parameters in mulberry and non-mulberry silk fibers," *Fibers and Polymer*, vol. 12, no. 4, pp. 499–505, 2011.

[10] M. I. Ivanova and L. Makowski, "Iterative low-pass filtering for estimation of the background in fiber diffraction patterns," *Acta Crystallographica A*, vol. 54, part 5, pp. 626–631, 1998.

[11] J. Squire, H. Al-khayat, S. Arnott et al., "New CCP13 software and strategy behind further developments: stripping and modelling of fibre diffraction data," *Fibre Diffraction Review*, vol. 11, pp. 7–19, 2003.

[12] K. Okuyama, K. Noguchi, T. Miyazawa, T. Yui, and K. Ogawa, "Molecular and crystal structure of hydrated chitosan," *Macromolecules*, vol. 30, no. 19, pp. 5849–5855, 1997.

[13] Y. Takahashi, M. Gehoh, and K. Yuzuriha, "Structure refinement and diffuse streak scattering of silk (*Bombyx mori*)," *International Journal of Biological Macromolecules*, vol. 24, no. 2-3, pp. 127–138, 1999.

[14] P. J. C. Smith and S. Arnott, "LALS: a linked-atom least-squares reciprocal-space refinement system incorporating stereochemical restraints to supplement sparse diffraction data," *Acta Crystallographica A*, vol. 34, pp. 3–11, 1978.

[15] L. Pauling and R. B. Corey, "The polypeptide-chain configuration in hbmoglobin and other globular proteins," *Proceedings of the National Academy of Sciences of the United States of America*, vol. 37, no. 5, pp. 282–285, 1951.

[16] L. Pauling and R. B. Corey, "Two pleated-sheet configurations of polypeptide chains involving both cis and trans amide groups," *Proceedings of the National Academy of Sciences of the United States of America*, vol. 39, no. 4, pp. 247–252, 1953.